PREPARED FOR SUBMISSION TO JHEP

Study of the $e^+e^- \to \pi^+\pi^- D_s^+ D_s^-$ process from $\sqrt{s} =$ 4.42 to 4.95 GeV at BESIII

BESIII Collaboration

M. Ablikim[1], M. N. Achasov[4,c], P. Adlarson[82], X. C. Ai[88], C. S. Akondi[31A,31B], R. Aliberti[39], A. Amoroso[81A,81C], Q. An[78,65,†], Y. H. An[88], M. S. Anderson[39], Y. Bai[63], O. Bakina[40], H. R. Bao[71], X. L. Bao[50], M. Barbagiovanni[81C], V. Batozskaya[1,49], K. Begzsuren[35], N. Berger[39], M. Berlowski[49], M. B. Bertani[30A], D. Bettoni[31A], F. Bianchi[81A,81C], E. Bianco[81A,81C], A. Bortone[81A,81C], I. Boyko[40], R. A. Briere[5], A. Brueggemann[75], D. Cabiati[81A,81C], H. Cai[83], M. H. Cai[42,k,l], X. Cai[1,65], A. Calcaterra[30A], G. F. Cao[1,71], N. Cao[1,71], S. A. Cetin[69A], X. Y. Chai[51,h], J. F. Chang[1,65], T. T. Chang[48], G. R. Che[48], Y. Z. Che[1,65,71], C. H. Chen[10], Chao Chen[1], G. Chen[1], H. S. Chen[1,71], H. Y. Chen[20], M. L. Chen[1,65,71], S. J. Chen[47], S. M. Chen[68], T. Chen[1,71], W. Chen[50], X. R. Chen[34,71], X. T. Chen[1,71], X. Y. Chen[12,g], Y. B. Chen[1,65], Y. Q. Chen[16], Z. K. Chen[66], J. Cheng[50], L. N. Cheng[48], S. K. Choi[11], X. Chu[12,g], G. Cibinetto[31A], F. Cossio[81C], J. Cottee-Meldrum[70], H. L. Dai[1,65], J. P. Dai[86], X. C. Dai[68], A. Dbeyssi[19], R. E. de Boer[3], D. Dedovich[40], C. Q. Deng[79], Z. Y. Deng[1], A. Denig[39], I. Denisenko[40], M. Destefanis[81A,81C], F. De Mori[81A,81C], E. Di Fiore[31A,31B], X. X. Ding[51,h], Y. Ding[44], Y. X. Ding[32], J. Dong[1,65], L. Y. Dong[1,71], M. Y. Dong[1,65,71], X. Dong[83], Z. J. Dong[66], M. C. Du[1], S. X. Du[88], Shaoxu Du[12,g], X. L. Du[12,g], Y. Q. Du[83], Y. Y. Duan[61], Z. H. Duan[47], P. Egorov[40,a], G. F. Fan[47], J. J. Fan[20], Y. H. Fan[50], J. Fang[1,65], Jin Fang[66], S. S. Fang[1,71], W. X. Fang[1], Y. Q. Fang[1,65,†], L. Fava[81B,81C], F. Feldbauer[3], G. Felici[30A], C. Q. Feng[78,65], J. H. Feng[16], Q. X. Feng[42,k,l], Y. T. Feng[78,65], M. Fritsch[3], C. D. Fu[1], J. L. Fu[71], Y. W. Fu[1,71], H. Gao[71], Xu Gao[38], Y. Gao[78,65], Y. N. Gao[51,h], Y. Y. Gao[32], Yunong Gao[20], Z. Gao[48], S. Garbolino[81C], I. Garzia[31A,31B], L. Ge[63], P. T. Ge[20], Z. W. Ge[47], C. Geng[66], A. Gilman[76], K. Goetzen[13], J. Gollub[3], J. B. Gong[1,71], J. D. Gong[38], L. Gong[44],

W. X. Gong[1,65], W. Gradl[39], M. Greco[81A,81C], M. D. Gu[56], M. H. Gu[1,65], C. Y. Guan[1,71], A. Q. Guo[34], H. Guo[55], J. N. Guo[12,g], L. B. Guo[46], M. J. Guo[55], R. P. Guo[54], X. Guo[55], Y. P. Guo[12,g], Z. Guo[78,65], A. Guskov[40,a], J. Gutierrez[29], J. Y. Han[78,65], T. T. Han[1], X. Han[78,65], F. Hanisch[3], K. D. Hao[78,65], X. Q. Hao[20], F. A. Harris[72], C. Z. He[51,h], K. K. He[17,47], K. L. He[1,71], F. H. Heinsius[3], C. H. Heinz[39], Y. K. Heng[1,65,71], C. Herold[67], P. C. Hong[38], G. Y. Hou[1,71], X. T. Hou[1,71], Y. R. Hou[71], Z. L. Hou[1], H. M. Hu[1,71], J. F. Hu[62,j], Q. P. Hu[78,65], S. L. Hu[12,g], T. Hu[1,65,71], Y. Hu[1], Y. X. Hu[83], Z. M. Hu[66], G. S. Huang[78,65], K. X. Huang[66], L. Q. Huang[34,71], P. Huang[47], X. T. Huang[55], Y. P. Huang[1], Y. S. Huang[66], T. Hussain[80], N. Hüsken[39], N. in der Wiesche[75], J. Jackson[29], Q. Ji[1], Q. P. Ji[20], W. Ji[1,71], X. B. Ji[1,71], X. L. Ji[1,65], Y. Y. Ji[1], L. K. Jia[71], X. Q. Jia[55], D. Jiang[1,71], S. J. Jiang[10], X. S. Jiang[1,65,71], Y. Jiang[71], J. B. Jiao[55], J. K. Jiao[38], Z. Jiao[25], L. C. L. Jin[1], S. Jin[47], Y. Jin[73], M. Q. Jing[56], X. M. Jing[71], T. Johansson[82], S. Kabana[36], X. L. Kang[10], X. S. Kang[44], B. C. Ke[88], V. Khachatryan[29], A. Khoukaz[75], O. B. Kolcu[69A], B. Kopf[3], L. Kröger[75], L. Krümmel[3], Y. Y. Kuang[79], X. Kui[1,71], N. Kumar[28], A. Kupsc[49,82], W. Kühn[41], Q. Lan[79], W. N. Lan[20], T. T. Lei[78,65], M. Lellmann[39], T. Lenz[39], C. Li[52], C. H. Li[46], C. K. Li[48], Chunkai Li[21], Cong Li[48], D. M. Li[88], F. Li[1,65], G. Li[1], H. B. Li[1,71], H. J. Li[20], H. L. Li[88], H. N. Li[62,j], H. P. Li[48], Hui Li[48], J. N. Li[32], J. S. Li[66], J. W. Li[55], K. Li[1], K. L. Li[42,k,l], L. J. Li[1,71], L. K. Li[26], Lei Li[53], M. H. Li[48], M. R. Li[1,71], M. T. Li[55], P. L. Li[71], P. R. Li[42,k,l], Q. M. Li[1,71], Q. X. Li[55], R. Li[18,34], S. Li[88], S. X. Li[88], S. Y. Li[88], Shanshan Li[27,i], T. Li[55], T. Y. Li[48], W. D. Li[1,71], W. G. Li[1,†], X. Li[1,71], X. H. Li[78,65], X. K. Li[51,h], X. L. Li[55], X. Y. Li[78,65], X. Z. Li[66], Y. Li[20], Y. H. Li[48], Y. B. Li[84], Y. C. Li[66], Y. G. Li[71], Y. P. Li[38], Z. H. Li[42], Z. J. Li[66], Z. L. Li[88], Z. X. Li[48], Z. Y. Li[86], C. Liang[47], H. Liang[78,65], Y. F. Liang[60], Y. T. Liang[34,71], Z. Z. Liang[66], G. R. Liao[14], L. B. Liao[66], M. H. Liao[66], Y. P. Liao[1,71], J. Libby[28], A. Limphirat[67], C. C. Lin[61], C. X. Lin[34], D. X. Lin[34,71], T. Lin[1], B. J. Liu[1], B. X. Liu[83], C. Liu[38], C. X. Liu[1], F. Liu[1], F. H. Liu[59], Feng Liu[6], G. M. Liu[62,j], H. Liu[42,k,l], H. B. Liu[15], H. M. Liu[1,71], Huihui Liu[22], J. B. Liu[78,65], J. J. Liu[21], K. Liu[42,k,l], K. Y. Liu[44], Ke Liu[23], Kun Liu[79], L. Liu[42], L. C. Liu[48], Lu Liu[48], M. H. Liu[38], P. L. Liu[55], Q. Liu[71], S. B. Liu[78,65], T. Liu[1], W. M. Liu[78,65], W. T. Liu[43], X. Liu[42,k,l], X. K. Liu[42,k,l], X. L. Liu[12,g], X. P. Liu[12,g], X. T. Liu[21], X. Y. Liu[83], Y. Liu[42,k,l], Y. B. Liu[48], Yi Liu[88], Z. A. Liu[1,65,71], Z. D. Liu[84], Z. L. Liu[79], Z. Q. Liu[55], Z. X. Liu[1], Z. Y. Liu[42], X. C. Lou[1,65,71], H. J. Lu[25], J. G. Lu[1,65], X. L. Lu[16], Y. Lu[7], Y. H. Lu[1,71], Y. P. Lu[1,65], Z. H. Lu[1,71], C. L. Luo[46], J. R. Luo[66], J. S. Luo[1,71], M. X. Luo[87], T. Luo[12,g], X. L. Luo[1,65], Z. Y. Lv[23], X. R. Lyu[71,o], Y. F. Lyu[48], Y. H. Lyu[88],

F. C. Ma[44], H. L. Ma[1], Heng Ma[27,i], J. L. Ma[1,71], L. L. Ma[55], L. R. Ma[73], Q. M. Ma[1], R. Q. Ma[1,71], R. Y. Ma[20], T. Ma[78,65], X. T. Ma[1,71], X. Y. Ma[1,65], F. E. Maas[19], I. MacKay[76], M. Maggiora[81A,81C], S. Maity[34], S. Malde[76], Y. J. Mao[51,h], Z. P. Mao[1], S. Marcello[81A,81C], A. Marshall[70], F. M. Melendi[31A,31B], Y. H. Meng[71], Z. X. Meng[73], G. Mezzadri[31A], H. Miao[1,71], T. J. Min[47], R. E. Mitchell[29], X. H. Mo[1,65,71], B. Moses[29], N. Yu. Muchnoi[4,c], J. Muskalla[39], Y. Nefedov[40], F. Nerling[19,e], H. Neuwirth[75], Z. Ning[1,65], S. Nisar[33], Q. L. Niu[42,k,l], W. D. Niu[12,g], Y. Niu[55], C. Normand[70], S. L. Olsen[11,71], Q. Ouyang[1,65,71], I. V. Ovtin[4], S. Pacetti[30B,30C], Y. Pan[63], A. Pathak[11], Y. P. Pei[78,65], M. Pelizaeus[3], G. L. Peng[78,65], H. P. Peng[78,65], X. J. Peng[42,k,l], Y. Y. Peng[42,k,l], K. Peters[13,e], K. Petridis[70], J. L. Ping[46], R. G. Ping[1,71], S. Plura[39], V. Prasad[38], L. Pöpping[3], F. Z. Qi[1], H. R. Qi[68], S. Qian[1,65], W. B. Qian[71], C. F. Qiao[71], J. H. Qiao[20], J. J. Qin[79], J. L. Qin[61], L. Q. Qin[14], L. Y. Qin[78,65], P. B. Qin[79], X. P. Qin[43], X. S. Qin[55], Z. H. Qin[1,65], J. F. Qiu[1], Z. H. Qu[79], J. Rademacker[70], K. Ravindran[74], C. F. Redmer[39], A. Rivetti[81C], M. Rolo[81C], G. Rong[1,71], S. S. Rong[1,71], F. Rosini[30B,30C], Ch. Rosner[19], M. Q. Ruan[1,65], W. R. Ruangyoo[67], N. Salone[49,q], A. Sarantsev[40,d], Y. Schelhaas[39], M. Schernau[36], K. Schoenning[82], M. Scodeggio[31A], W. Shan[26], X. Y. Shan[78,65], Z. J. Shang[42,k,l], J. F. Shangguan[17], L. G. Shao[1,71], M. Shao[78,65], C. P. Shen[12,g], H. F. Shen[1,9], W. H. Shen[71], X. Y. Shen[1,71], B. A. Shi[71], Ch. Y. Shi[86,b], H. Shi[78,65], J. L. Shi[8,p], J. Y. Shi[1], M. H. Shi[88], S. Y. Shi[79], X. Shi[1,65], H. L. Song[78,65], J. J. Song[20], M. H. Song[42], T. Z. Song[66], W. M. Song[38], Y. X. Song[51,h,m], Zirong Song[27,i], S. Sosio[81A,81C], S. Spataro[81A,81C], S. Stansilaus[76], F. Stieler[39], M. Stolte[3], S. S Su[44], G. B. Sun[83], G. X. Sun[1], H. Sun[71], H. K. Sun[1], J. F. Sun[20], K. Sun[68], L. Sun[83], R. Sun[78], S. S. Sun[1,71], T. Sun[57,f], W. Y. Sun[56], Y. C. Sun[83], Y. H. Sun[32], Y. J. Sun[78,65], Y. Z. Sun[1], Z. Q. Sun[1,71], Z. T. Sun[55], H. Tabaharizato[1], N. T. Tagsinsit[67], C. J. Tang[60], G. Y. Tang[1], J. Tang[66], J. J. Tang[78,65], L. F. Tang[43], Y. A. Tang[83], Z. H. Tang[1,71], L. Y. Tao[79], M. Tat[76], J. X. Teng[78,65], J. Y. Tian[78,65], W. H. Tian[66], Y. Tian[34], Z. F. Tian[83], K. Yu. Todyshev[4], I. Uman[69B], E. van der Smagt[3], B. Wang[66], Bin Wang[1], Bo Wang[78,65], C. Wang[42,k,l], Chao Wang[20], Cong Wang[23], D. Y. Wang[51,h], F. K. Wang[66], H. J. Wang[42,k,l], H. R. Wang[85], J. Wang[10], J. J. Wang[83], J. P. Wang[37], K. Wang[1,65], L. L. Wang[1], L. W. Wang[38], M. Wang[55], Mi Wang[78,65], N. Y. Wang[71], P. Wang[21], S. Wang[42,k,l], Shun Wang[64], T. Wang[12,g], W. Wang[66], W. P. Wang[39], X. F. Wang[42,k,l], X. L. Wang[12,g], X. N. Wang[1,71], Xin Wang[27,i], Y. Wang[1], Y. D. Wang[50], Y. F. Wang[1,9,71], Y. H. Wang[42,k,l], Y. J. Wang[78,65], Y. L. Wang[20], Y. N. Wang[50], Yanning Wang[83], Yaqian Wang[18], Yi Wang[68], Yuan Wang[18,34], Z. Wang[1,65], Z. L. Wang[2], Z. Q. Wang[12,g], Z. Y. Wang[1,71], Zhi Wang[48], Ziyi Wang[71], D. Wei[48], D. H. Wei[14], D. J. Wei[73], H. R. Wei[48], F. Weidner[75], H. R. Wen[34], S. P. Wen[1], U. Wiedner[3], G. Wilkinson[76], M. Wolke[82], J. F. Wu[1,9], L. H. Wu[1], L. J. Wu[20], Lianjie Wu[20], S. G. Wu[1,71], S. M. Wu[71], X. W. Wu[79], Z. Wu[1,65], H. L. Xia[78,65], L. Xia[78,65], B. H. Xiang[1,71], D. Xiao[42,k,l], G. Y. Xiao[47], H. Xiao[79], Y. L. Xiao[12,g], Z. J. Xiao[46], C. Xie[47], K. J. Xie[1,71], Y. Xie[55], Y. G. Xie[1,65], Y. H. Xie[6], Z. P. Xie[78,65], T. Y. Xing[1,71], D. B. Xiong[1], G. F. Xu[1], H. Y. Xu[2], Q. J. Xu[17], Q. N. Xu[32], T. D. Xu[79], X. P. Xu[61], Y. Xu[12,g], Y. C. Xu[85], Z. S. Xu[71], F. Yan[24], L. Yan[12,g], W. B. Yan[78,65], W. C. Yan[88], W. H. Yan[6], W. P. Yan[20], X. Q. Yan[12,g], Y. Y. Yan[67], H. J. Yang[57,f], H. L. Yang[38], H. X. Yang[1], J. H. Yang[47], R. J. Yang[20], X. Y. Yang[73], Y. Yang[12,g], Y. G. Yang[56], Y. H. Yang[48], Y. M. Yang[88], Y. Q. Yang[10], Y. Z. Yang[20], Youhua Yang[47], Z. Y. Yang[79], W. J. Yao[6], Z. P. Yao[55], M. Ye[1,65], M. H. Ye[9,†], Z. J. Ye[62,j], K. Yi[46], Junhao Yin[48], Z. Y. You[66], B. X. Yu[1,65,71], C. X. Yu[48], G. Yu[13], J. S. Yu[27,i], L. W. Yu[12,g], T. Yu[79], X. D. Yu[51,h], Y. C. Yu[88], Yongchao Yu[42], C. Z. Yuan[1,71], H. Yuan[1,71], J. Yuan[38], Jie Yuan[50], L. Yuan[2], M. K. Yuan[12,g], S. H. Yuan[79], Y. Yuan[1,71], C. X. Yue[43], Ying Yue[20], A. A. Zafar[80], F. R. Zeng[55], S. H. Zeng[70], X. Zeng[12,g], Y. J. Zeng[1,71], Yujie Zeng[66], Y. C. Zhai[55], Y. H. Zhan[66], B. L. Zhang[1,71], B. X. Zhang[1,†], D. H. Zhang[48], G. Y. Zhang[20], Gengyuan Zhang[1,71], H. Zhang[78,65], H. C. Zhang[1,65,71], H. H. Zhang[66], H. Q. Zhang[1,65,71], H. R. Zhang[78,65], H. Y. Zhang[1,65], Han Zhang[88], J. Zhang[66], J. J. Zhang[58], J. L. Zhang[21], J. Q. Zhang[46], J. S. Zhang[12,g], J. W. Zhang[1,65,71], J. X. Zhang[42,k,l], J. Y. Zhang[1], J. Z. Zhang[1,71], Jianyu Zhang[71], Jin Zhang[53], Jiyuan Zhang[12,g], L. M. Zhang[68], Lei Zhang[47], N. Zhang[38], P. Zhang[1,9], Q. Zhang[20], Q. Y. Zhang[38], Q. Z. Zhang[71], R. Y. Zhang[42,k,l], S. H. Zhang[1,71], S. N. Zhang[76], Shulei Zhang[27,i], X. M. Zhang[1], X. Y. Zhang[55], Y. T. Zhang[88], Y. H. Zhang[1,65], Y. P. Zhang[78,65], Yao Zhang[1], Yu Zhang[79], Yu Zhang[66], Z. Zhang[34], Z. D. Zhang[1], Z. H. Zhang[1], Z. L. Zhang[38], Z. X. Zhang[20], Z. Y. Zhang[83], Zh. Zh. Zhang[20], Zhilong Zhang[61], Ziyang Zhang[50], Ziyu Zhang[48], G. Zhao[1], J.-P. Zhao[71], J. Y. Zhao[1,71], J. Z. Zhao[1,65], L. Zhao[1], Lei Zhao[78,65], M. G. Zhao[48], R. P. Zhao[71], S. J. Zhao[88], Y. B. Zhao[1,65], Y. L. Zhao[61], Y. P. Zhao[50], Y. X. Zhao[34,71], Z. G. Zhao[78,65], A. Zhemchugov[40,a], B. Zheng[79], B. M. Zheng[38], J. P. Zheng[1,65], W. J. Zheng[1,71], W. Q. Zheng[10], X. R. Zheng[20], Y. H. Zheng[71,o], B. Zhong[46], C. Zhong[20], X. Zhong[45], H. Zhou[39,55,n], J. Q. Zhou[38], S. Zhou[6], X. Zhou[83], X. K. Zhou[6], X. R. Zhou[78,65], X. Y. Zhou[43], Y. X. Zhou[85], Y. Z. Zhou[20], A. N. Zhu[71], J. Zhu[48], K. Zhu[1], K. J. Zhu[1,65,71], K. S. Zhu[12,g], L. X. Zhu[71], Lin Zhu[20], S. H. Zhu[77],

T. J. Zhu[12,g], W. D. Zhu[12,g], W. J. Zhu[1], W. Z. Zhu[20], Y. C. Zhu[78,65], Z. A. Zhu[1,71], X. Y. Zhuang[48], M. Zhuge[55], J. H. Zou[1], J. Zu[34]

(BESIII Collaboration)

[1] *Institute of High Energy Physics, Beijing 100049, People's Republic of China*
[2] *Beihang University, Beijing 100191, People's Republic of China*
[3] *Bochum Ruhr-University, D-44780 Bochum, Germany*
[4] *Budker Institute of Nuclear Physics SB RAS (BINP), Novosibirsk 630090, Russia*
[5] *Carnegie Mellon University, Pittsburgh, Pennsylvania 15213, USA*
[6] *Central China Normal University, Wuhan 430079, People's Republic of China*
[7] *Central South University, Changsha 410083, People's Republic of China*
[8] *Chengdu University of Technology, Chengdu 610059, People's Republic of China*
[9] *China Center of Advanced Science and Technology, Beijing 100190, People's Republic of China*
[10] *China University of Geosciences, Wuhan 430074, People's Republic of China*
[11] *Chung-Ang University, Seoul, 06974, Republic of Korea*
[12] *Fudan University, Shanghai 200433, People's Republic of China*
[13] *GSI Helmholtzcentre for Heavy Ion Research GmbH, D-64291 Darmstadt, Germany*
[14] *Guangxi Normal University, Guilin 541004, People's Republic of China*
[15] *Guangxi University, Nanning 530004, People's Republic of China*
[16] *Guangxi University of Science and Technology, Liuzhou 545006, People's Republic of China*
[17] *Hangzhou Normal University, Hangzhou 310036, People's Republic of China*
[18] *Hebei University, Baoding 071002, People's Republic of China*
[19] *Helmholtz Institute Mainz, Staudinger Weg 18, D-55099 Mainz, Germany*
[20] *Henan Normal University, Xinxiang 453007, People's Republic of China*
[21] *Henan University, Kaifeng 475004, People's Republic of China*
[22] *Henan University of Science and Technology, Luoyang 471003, People's Republic of China*
[23] *Henan University of Technology, Zhengzhou 450001, People's Republic of China*
[24] *Hengyang Normal University, Hengyang 421002, People's Republic of China*
[25] *Huangshan College, Huangshan 245000, People's Republic of China*
[26] *Hunan Normal University, Changsha 410081, People's Republic of China*
[27] *Hunan University, Changsha 410082, People's Republic of China*
[28] *Indian Institute of Technology Madras, Chennai 600036, India*
[29] *Indiana University, Bloomington, Indiana 47405, USA*
[30] *INFN Laboratori Nazionali di Frascati, (A)INFN Laboratori Nazionali di Frascati, I-00044, Frascati, Italy; (B)INFN Sezione di Perugia, I-06100, Perugia, Italy; (C)University of Perugia, I-06100, Perugia, Italy*
[31] *INFN Sezione di Ferrara, (A)INFN Sezione di Ferrara, I-44122, Ferrara, Italy; (B)University of Ferrara, I-44122, Ferrara, Italy*
[32] *Inner Mongolia University, Hohhot 010021, People's Republic of China*
[33] *Institute of Business Administration, University Road, Karachi, 75270 Pakistan*

[34] *Institute of Modern Physics, Lanzhou 730000, People's Republic of China*
[35] *Institute of Physics and Technology, Mongolian Academy of Sciences, Peace Avenue 54B, Ulaanbaatar 13330, Mongolia*
[36] *Instituto de Alta Investigación, Universidad de Tarapacá, Casilla 7D, Arica 1000000, Chile*
[37] *Jiangsu Ocean University, Lianyungang 222000, People's Republic of China*
[38] *Jilin University, Changchun 130012, People's Republic of China*
[39] *Johannes Gutenberg University of Mainz, Johann-Joachim-Becher-Weg 45, D-55099 Mainz, Germany*
[40] *Joint Institute for Nuclear Research, 141980 Dubna, Moscow region, Russia*
[41] *Justus-Liebig-Universitaet Giessen, II. Physikalisches Institut, Heinrich-Buff-Ring 16, D-35392 Giessen, Germany*
[42] *Lanzhou University, Lanzhou 730000, People's Republic of China*
[43] *Liaoning Normal University, Dalian 116029, People's Republic of China*
[44] *Liaoning University, Shenyang 110036, People's Republic of China*
[45] *Longyan University, Longyan 364000, People's Republic of China*
[46] *Nanjing Normal University, Nanjing 210023, People's Republic of China*
[47] *Nanjing University, Nanjing 210093, People's Republic of China*
[48] *Nankai University, Tianjin 300071, People's Republic of China*
[49] *National Centre for Nuclear Research, Warsaw 02-093, Poland*
[50] *North China Electric Power University, Beijing 102206, People's Republic of China*
[51] *Peking University, Beijing 100871, People's Republic of China*
[52] *Qufu Normal University, Qufu 273165, People's Republic of China*
[53] *Renmin University of China, Beijing 100872, People's Republic of China*
[54] *Shandong Normal University, Jinan 250014, People's Republic of China*
[55] *Shandong University, Jinan 250100, People's Republic of China*
[56] *Shandong University of Technology, Zibo 255000, People's Republic of China*
[57] *Shanghai Jiao Tong University, Shanghai 200240, People's Republic of China*
[58] *Shanxi Normal University, Linfen 041004, People's Republic of China*
[59] *Shanxi University, Taiyuan 030006, People's Republic of China*
[60] *Sichuan University, Chengdu 610064, People's Republic of China*
[61] *Soochow University, Suzhou 215006, People's Republic of China*
[62] *South China Normal University, Guangzhou 510006, People's Republic of China*
[63] *Southeast University, Nanjing 211100, People's Republic of China*
[64] *Southwest University of Science and Technology, Mianyang 621010, People's Republic of China*
[65] *State Key Laboratory of Particle Detection and Electronics, Beijing 100049, Hefei 230026, People's Republic of China*
[66] *Sun Yat-Sen University, Guangzhou 510275, People's Republic of China*
[67] *Suranaree University of Technology, University Avenue 111, Nakhon Ratchasima 30000, Thailand*
[68] *Tsinghua University, Beijing 100084, People's Republic of China*
[69] *Turkish Accelerator Center Particle Factory Group, (A)Istinye University, 34010,*

Istanbul, Turkey; (B)Near East University, Nicosia, North Cyprus, 99138, Mersin 10, Turkey
[70] *University of Bristol, H H Wills Physics Laboratory, Tyndall Avenue, Bristol, BS8 1TL, UK*
[71] *University of Chinese Academy of Sciences, Beijing 100049, People's Republic of China*
[72] *University of Hawaii, Honolulu, Hawaii 96822, USA*
[73] *University of Jinan, Jinan 250022, People's Republic of China*
[74] *University of La Serena, Av. Raúl Bitrán 1305, La Serena, Chile*
[75] *University of Muenster, Wilhelm-Klemm-Strasse 9, 48149 Muenster, Germany*
[76] *University of Oxford, Keble Road, Oxford OX13RH, United Kingdom*
[77] *University of Science and Technology Liaoning, Anshan 114051, People's Republic of China*
[78] *University of Science and Technology of China, Hefei 230026, People's Republic of China*
[79] *University of South China, Hengyang 421001, People's Republic of China*
[80] *University of the Punjab, Lahore-54590, Pakistan*
[81] *University of Turin and INFN, (A)University of Turin, I-10125, Turin, Italy; (B)University of Eastern Piedmont, I-15121, Alessandria, Italy; (C)INFN, I-10125, Turin, Italy*
[82] *Uppsala University, Box 516, SE-75120 Uppsala, Sweden*
[83] *Wuhan University, Wuhan 430072, People's Republic of China*
[84] *Xi'an Jiaotong University, No.28 Xianning West Road, Xi'an, Shaanxi 710049, P.R. China*
[85] *Yantai University, Yantai 264005, People's Republic of China*
[86] *Yunnan University, Kunming 650500, People's Republic of China*
[87] *Zhejiang University, Hangzhou 310027, People's Republic of China*
[88] *Zhengzhou University, Zhengzhou 450001, People's Republic of China*

[†] *Deceased*
[a] *Also at the Moscow Institute of Physics and Technology, Moscow 141700, Russia*
[b] *Also at the Functional Electronics Laboratory, Tomsk State University, Tomsk, 634050, Russia*
[c] *Also at the Novosibirsk State University, Novosibirsk, 630090, Russia*
[d] *Also at the NRC "Kurchatov Institute", PNPI, 188300, Gatchina, Russia*
[e] *Also at Goethe University Frankfurt, 60323 Frankfurt am Main, Germany*
[f] *Also at Key Laboratory for Particle Physics, Astrophysics and Cosmology, Ministry of Education; Shanghai Key Laboratory for Particle Physics and Cosmology; Institute of Nuclear and Particle Physics, Shanghai 200240, People's Republic of China*
[g] *Also at Key Laboratory of Nuclear Physics and Ion-beam Application (MOE) and Institute of Modern Physics, Fudan University, Shanghai 200443, People's Republic of China*
[h] *Also at State Key Laboratory of Nuclear Physics and Technology, Peking University, Beijing 100871, People's Republic of China*

[i] *Also at School of Physics and Electronics, Hunan University, Changsha 410082, China*
[j] *Also at Guangdong Provincial Key Laboratory of Nuclear Science, Institute of Quantum Matter, South China Normal University, Guangzhou 510006, China*
[k] *Also at MOE Frontiers Science Center for Rare Isotopes, Lanzhou University, Lanzhou 730000, People's Republic of China*
[l] *Also at Lanzhou Center for Theoretical Physics, Lanzhou University, Lanzhou 730000, People's Republic of China*
[m] *Also at Ecole Polytechnique Federale de Lausanne (EPFL), CH-1015 Lausanne, Switzerland*
[n] *Also at Helmholtz Institute Mainz, Staudinger Weg 18, D-55099 Mainz, Germany*
[o] *Also at Hangzhou Institute for Advanced Study, University of Chinese Academy of Sciences, Hangzhou 310024, China*
[p] *Also at Applied Nuclear Technology in Geosciences Key Laboratory of Sichuan Province, Chengdu University of Technology, Chengdu 610059, People's Republic of China*
[q] *Currently at University of Silesia in Katowice, Institute of Physics, 75 Pulku Piechoty 1, 41-500 Chorzow, Poland*

ABSTRACT: Based on 8.5 fb^{-1} of e^+e^- collision data collected at center-of-mass energies between 4.42 and 4.95 GeV with the BESIII detector at the BEPCII storage ring, we investigate the process $e^+e^- \to \pi^+\pi^- D_s^+ D_s^-$. With no significant signal observed, upper limits on the Born cross sections of $e^+e^- \to \pi^+\pi^- D_s^+ D_s^-$ at each energy value at the 90% confidence level are determined. Additionally, a search for intermediate charmonium-like resonances is performed in the $M(D_s^+ D_s^-)$ invariant mass spectrum, but no significant resonant structures are observed with the current statistics.

Contents

1 Introduction

In recent years, the exploration of charmonium-like states has become a prominent focus in hadron physics. Vector charmonium-like states with masses above the open-charm threshold, as for example $Y(4230)$, $Y(4360)$ and $Y(4660)$, have been observed in many experiments, including BABAR [1–4], Belle [5–8], CLEO [9, 10], and BESIII [11–13]. A thorough investigation of these states in the open-charm channel can provide crucial insights into their characteristics and test different theoretical explanations such as hybrid charmonium [14], tetraquark [15], and hadronic molecule [16, 17] models.

The BESIII experiment has identified various charmonium-like states in open-charm processes, including $Y(4220)$, $Y(4390)$ [18], $Z_c(3900)$ [19]. In 2021, BESIII announced the observation of a novel exotic multi-quark state candidate, $Z_{cs}(3985)^-$, produced in the reaction $e^+e^- \to K^+(D_s^-D^{*0} + D_s^{*-}D^0)$; the production occurred at the center-of-mass (c.m.) energy ($\sqrt{s}$) of 4.68 GeV [20]. The revelation of $Z_{cs}(3985)^-$ has stimulated a fresh wave of investigations into multi-quark structures. Researchers are particularly focusing on the interplay between charm and strange quarks within these states. Recently, the LHCb experiment unveiled a distinct and intriguing hadronic state in the $D_s^+D_s^-$ system originating from the three-body decay $B^+ \to D_s^+D_s^-K^+$, which indicates the potential presence of a four-quark ($c\bar{c}s\bar{s}$) element [21].

In this analysis, we investigate the process $e^+e^- \to \pi^+\pi^-D_s^+D_s^-$, focusing on the interactions of the two $D_s^\pm$ mesons, which are charm-strange quark bound states. By analyzing data from the BESIII detector at c.m. energies ranging from 4.42 to 4.95 GeV [22, 23], we measure the Born cross sections. This study aims to enhance our understanding of charm and strange quark dynamics in multi-quark systems, and provide insights into the structures composed of charm and strange quarks [24, 25].

2 Detector and Data Samples

The BESIII detector [26] records symmetric e^+e^- collisions provided by the BEPCII storage ring [27] in the c.m. energies range from 1.84 to 4.95 GeV, with a peak luminosity of 1.1×10^{33} cm^{-2}s^{-1} achieved at $\sqrt{s} = 3.773$ GeV. BESIII has collected large data samples in this energy region [28–30].

The cylindrical core of the BESIII detector covers 93% of the full solid angle and consists of a helium-based multilayer drift chamber (MDC), a time-of-flight system (TOF), and a CsI(Tl) electromagnetic calorimeter (EMC), which are all enclosed in a superconducting solenoidal magnet providing a 1.0 T magnetic field. The solenoid is supported by an octagonal flux-return yoke with resistive plate counter muon identification modules interleaved with steel. The charged-particle momentum resolution at 1 GeV/c is 0.5%, and the dE/dx resolution is 6% for electrons from Bhabha scattering. The EMC measures photon energies with a resolution of 2.5% (5%) at 1 GeV in the barrel (end cap) region. The time resolution of the TOF barrel part is 68 ps, and the end-cap TOF system was upgraded in 2015 with a multi-gap resistive plate chamber technology, providing a time resolution of 60 ps, which benefits 73% of the data used in this analysis [31–33].

The analysis is performed within the framework of the BESIII Offline Software System (BOSS) [34] which handles detector calibration, event reconstruction and data storage. The dataset comprises data samples at 15 energy values. The integrated luminosities are determined through large-angle Bhabha events, and the c.m. energies of the data samples are obtained from offline measurements [23]. Monte Carlo (MC) simulations are employed to determine detection efficiencies and estimate backgrounds. They are generated with a GEANT4-based [35] software package, which includes the geometric description of the BESIII detector and the detector response, are used to determine detection efficiencies and to estimate backgrounds. The simulation models the beam energy spread and initial state radiation (ISR) in e^+e^- annihilations using the KKMC generator [36]. Inclusive MC samples for background assessments are generated in a range of $\sqrt{s} = 4.42$ to 4.95 GeV. All particle decays are modelled with EVTGEN [37, 38] using branching fractions either taken from the Particle Data Group (PDG) [39], when available, or otherwise estimated with LUNDCHARM [40].

The signal processes involve the $e^+e^- \to \pi^+\pi^- D_s^+ D_s^-$ reaction, where the decays are generated by BesEvtGen, including $D_s^+ \to K_S^0 K^+$ and $K^+K^-\pi^+$, $D_s^- \to K_S^0 K^-$ and $K^+K^-\pi^-$. The decays of $D_s^+ \to K_S^0 K^+$ and $D_s^- \to K_S^0 K^-$ follow the phase space model (PHSP), while $D_s^+ \to K^+K^-\pi^+$ and $D_s^- \to K^+K^-\pi^-$ adhere to the D_DALITZ [38, 41] model.

3 Event Selections and Analysis Techniques

A full reconstruction method is used to extract the signal process $e^+e^- \to \pi^+\pi^- D_s^+ D_s^-$, where the $D_s^\pm$ mesons decay into $K^+K^-\pi^\pm$ or $K_S^0(\to \pi^+\pi^-)K^\pm$. Charged tracks are reconstructed from MDC hits within a polar-angle (θ) acceptance range of $|\cos\theta| < 0.93$, where θ is defined with respect to the symmetry axis of the MDC (defined as the z-axis). For the charged tracks not originating from K_S^0 decays, the distance of the closest approach to the interaction point (IP) must be less than 10 cm along the z-axis (V_z), and less than 1 cm in the transverse plane (V_{xy}). The $\mathrm{d}E/\mathrm{d}x$ and TOF information for each charged track are combined to calculate the Particle Identification (PID) probabilities P_i ($i = \pi, K$) for each particle-type hypothesis. Kaon candidates are required to have $P_K > P_\pi$, while pion candidates must satisfy $P_\pi > P_K$.

Each K_S^0 candidate is reconstructed from two oppositely charged tracks satisfying the conditions $|V_z| < 20$ cm and $|\cos\theta| < 0.93$. The two charged tracks are assigned as $\pi^+\pi^-$ without imposing PID criteria. They are constrained to originate from a common vertex and are required to have an invariant mass ($M_{\pi^+\pi^-}$) within the interval (0.487, 0.511) GeV/c^2. The decay length of the K_S^0 candidate is required to be greater than twice the vertex resolution.

Selected $K^\pm$, $\pi^\pm$, K_S^0 candidates are used to reconstruct the $D_s^\pm$ meson candidates. For events with multiple candidate combinations, the optimal pair is selected by minimizing the variable $\Delta\hat{M} = |\hat{M} - M_{\rm PDG}(D_s^\pm)|$, where $\hat{M} = [M(D_s^+) + M(D_s^-)]/2$ is the average reconstructed mass of the $D_s^+D_s^-$ pair, and $M_{\rm PDG}(D_s^\pm)$ is the nominal mass from the PDG [39].

In order to suppress backgrounds, mass window requirements for the intermediate states ϕ and $\overline{K}^{*0}$ are applied during the $D_s^+ \to K^-K^+\pi^+$ candidate selection. Based on the observed invariant mass distributions of $M(K^+K^-)$ and $M(K^-\pi^+)$ as shown in Fig. 1, the mass window for the ϕ in the $D_s^+ \to \phi\pi^+$ decay is required to be $M(K^+K^-) < 1.2$ GeV/c^2. Similarly, for the $\overline{K}^{*0}$ in $D_s^+ \to \overline{K}^{*0}K^+$, the mass window is set as $M(K^-\pi^+) < 1.0$ GeV/c^2. Corresponding selection criteria are also applied to the D_s^- candidates.

The inclusive MC samples are utilized to examine potential background contributions. After applying all the specified requirements, a total of 73 events remain. All of them are non-dominant backgrounds, and no significant peaking background is observed within the $D_s^\pm$ signal region.

4 Signal Extraction

The signal yield at each energy point is obtained by performing a one-dimensional (1D) unbinned maximum likelihood fit to the corresponding $RM(\pi^+\pi^-D_s^\pm)$ distribution. The mass window requirement $|M(D_s^-) - M_{\rm PDG}(D_s^-)| < 15$ MeV/c^2 is applied in the fit to the $RM(\pi^+\pi^-D_s^-)$ distribution, and similarly for the $RM(\pi^+\pi^-D_s^+)$ fit. To improve the mass resolution, the corrected recoil mass $RM(\pi^+\pi^-D_s^+) + M(D_s^+) - M_{\rm PDG}(D_s^+)$ is used. The signal shape is modeled by a non-parametric PDF, which is a histogram-based PDF that describes the signal shape by interpolating the distribution of the simulated

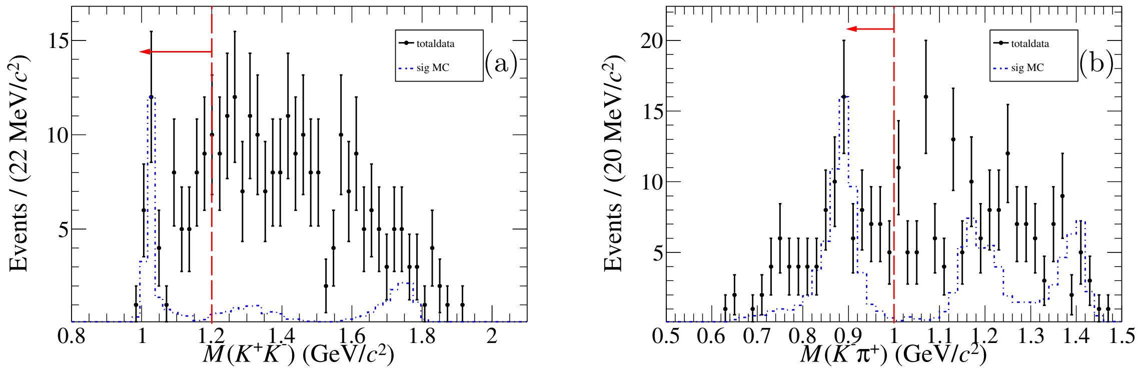

FIG 1. The invariant mass of $M(K^+K^-)$ (a) and $M(K^-\pi^+)$ (b). The black dots with error bars represent the data for fifteen energy points, the solid lines (blue) describe the signal MC at $\sqrt{s} = 4.42$ GeV.

MC events. Meanwhile, a first-order polynomial function models the background shape. In the fitting process, both the signal and background yields, as well as the polynomial function parameters for the background shape, are floated. The data from the fifteen samples are combined to enhance the statistical significance. The fits to the $RM(\pi^+\pi^-D_s^+)$ and $RM(\pi^+\pi^-D_s^-)$ distributions are illustrated in Fig. 2. The χ^2/NDF values are 1.3/2 for $RM(\pi^+\pi^-D_s^+)$ and 4.1/3 for $RM(\pi^+\pi^-D_s^-)$. The signal yields in the $RM(\pi^+\pi^-D_s^+)$ and $RM(\pi^+\pi^-D_s^-)$ fits are $4.7^{+6.4}_{-3.3}$ and $11.2^{+7.6}_{-5.2}$, respectively. The statistical significance of the signal is determined to be 1.2σ and 2.6σ by comparing the likelihood values with and without the signal assumption in the fits, considering the change in degrees of freedom. For a conservative estimation of the significance, the outcome from the fit to $RM(\pi^+\pi^-D_s^+)$ is chosen as the nominal result.

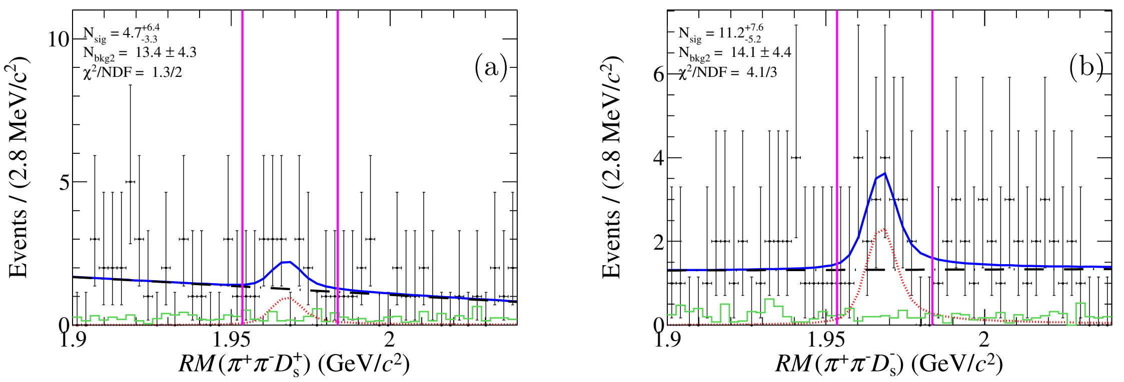

FIG 2. Fits to the $RM(\pi^+\pi^-D_s^+)$ and $RM(\pi^+\pi^-D_s^-)$ distributions in (a) and (b), respectively. The black dots with error bars represent data, the solid blue lines show the total fits, the dashed red lines indicate the signal shapes, the green line shows the background from inclusive MC after scaling, and the dash-dotted black lines represent the background.

5 Search for the Charmonium-like States in the $D_s^+ D_s^-$ System

To explore potential charmonium-like intermediate states, the $M(D_s^+ D_s^-)$ invariant mass spectrum is examined using the combined data samples from all fifteen energy values, corresponding to a total integrated luminosity of 8.5 fb^{-1}. As shown in Fig. 3, the $M(D_s^+ D_s^-)$ distribution is compared with the PHSP MC component. The PHSP MC shape (blue dashed line) is obtained by combining the PHSP MC samples from each energy value, weighted by their respective measured Born cross sections, selection efficiencies, and integrated luminosities. To reduce statistical fluctuations, the weighted PHSP MC distribution is further smoothed.

No significant resonant structures are observed in the $M(D_s^+ D_s^-)$ system with the current data sample, and the result remains statistically limited.

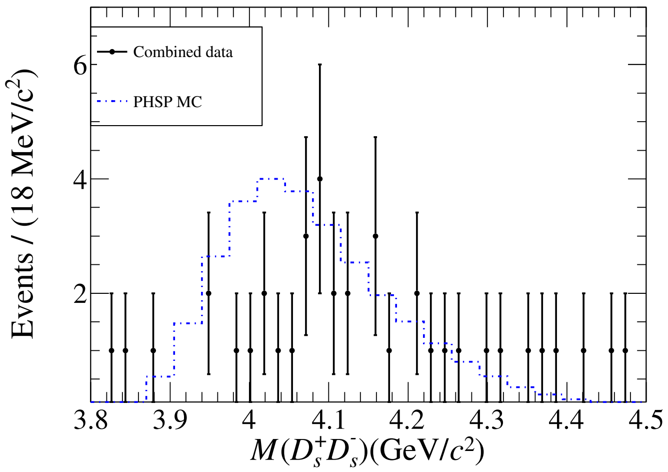

FIG 3. The $M(D_s^+ D_s^-)$ invariant mass distribution for the combined data samples. The black dots with error bars represent data, and the dotted blue curve shows the weighted PHSP component.

6 Born Cross Section Measurement

The Born cross section for the process $e^+e^- \to \pi^+\pi^- D_s^+ D_s^-$ can be calculated as follows

$$\sigma(e^+e^- \to \pi^+\pi^- D_s^+ D_s^-) = \frac{N^{\rm sig}}{\mathcal{L}(1+\delta^r)(1+\delta^v)\sum_{i,j}\epsilon_{ij}\mathcal{B}_i\mathcal{B}_j}, \tag{6.1}$$

where $N^{\rm sig}$ is the signal yield, $\mathcal{L}$ is the integrated luminosity [23], ϵ_{ij} indicates the signal efficiency for $e^+e^- \to \pi^+\pi^- D_s^+ D_s^-$ with $D_s^+ \to i$ and $D_s^- \to j$; $\mathcal{B}_i$ and $\mathcal{B}_j$ are the branching fractions for $D_s^+ \to i$ and $D_s^- \to j$, respectively; $1+\delta^r$ is the ISR correction factor, which is defined as

$$1+\delta^r = \frac{\sigma^{\rm obs}}{\sigma^B} = \frac{\int \sigma^B(s(1-x))F(x,s)dx}{\sigma^B(s)}, \tag{6.2}$$

where $F(x,s)$ is the radiator function derived from QED calculations [42] with 0.1% accuracy. The input line shape σ^B in Eq. (6.2) is parameterized by a cubic polynomial function fitted to the initially measured Born cross sections. This line shape is then used to determine the final ISR correction factors and efficiencies for all data samples. The factor $1+\delta^v$ is the vacuum polarization (VP) correction factor calculated using the Fortran package provided by Fred Jegerlehner [43], which determines the correction by summing the leptonic contribution calculated in precise perturbative QED and the non-perturbative hadronic contribution evaluated via dispersion relations using experimental data for electron-positron annihilation into hadrons. Figure 4 shows the measured Born cross sections and their upper limits obtained from this analysis (blue dots).

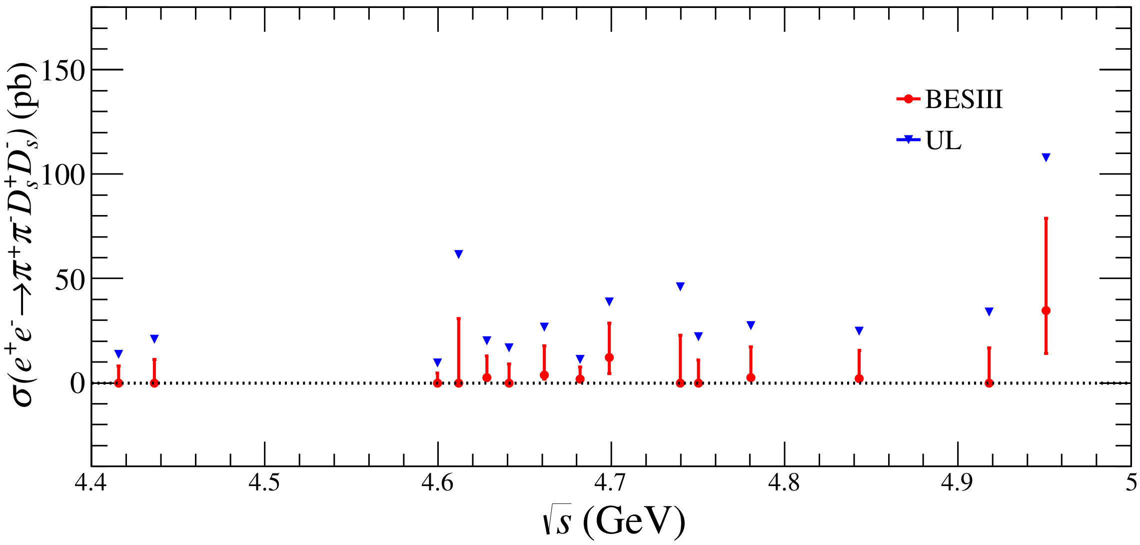

FIG 4. Born cross sections of $e^+e^- \to \pi^+\pi^- D_s^+ D_s^-$ at different center-of-mass energies. The red dots with error bars represent the measurements from this analysis, while the blue triangles indicate the upper limits.

7 Systematic Uncertainties

Systematic uncertainties are mainly from the luminosity measurement, the quoted branching fractions, the ISR correction factor, and the fit schemes. Due to the limited statistics and large fluctuations at individual energy points, the systematic uncertainties are evaluated using the combined data sample when applicable, in order to obtain a stable estimate. For this purpose, the average Born cross section is calculated as

$$\bar{\sigma}(e^+e^- \to \pi^+\pi^- D_s^+ D_s^-) = \frac{N_{\text{tot}}}{\sum_k \left[\mathcal{L}_k(1+\delta_k^r)(1+\delta_k^v)\sum_{i,j}\epsilon_{ij}^{(k)}\mathcal{B}_i\mathcal{B}_j\right]}, \tag{7.1}$$

where N_{tot} is the total signal yield across all fifteen energy values, $\mathcal{L}_k$ is the integrated luminosity of the k-th energy value, $1+\delta_k^r$ and $1+\delta_k^v$ are the ISR correction factor and the

VP correction factor at the k-th energy value, respectively. A summary of the systematic uncertainties is given in TABLE 1. The total systematic uncertainty is obtained by summing the individual contributions in quadrature.

The integrated luminosities of these data samples are measured using Bhabha events, with an uncertainty of 1.0% [44].

The systematic uncertainty due to the charged π and K tracking from the interaction point (IP) is estimated to be 1.0% per track [45–47]. The detection efficiencies are varied within one standard deviation according to the charged track multiplicities in the $D_s^\pm$ reconstruction channels; the largest difference in the cross sections, 7.0%, is taken as the systematic uncertainty. Similarly, the systematic uncertainty due to PID is taken to be 1.0% per charged track [45–47]. The systematic uncertainty associated with K_S^0 reconstruction is taken as 0.4% [48].

The branching fractions of $D_s^+ \to K_S^0 K^+$ and $D_s^+ \to K^+ K^- \pi^+$ are taken from the PDG [39]. Their uncertainties are propagated to the final cross section measurement by varying the branching fractions by $\pm 1\sigma$ in the calculation. The resulting largest differences from the nominal cross sections are assigned as the systematic uncertainties, which are determined to be 0.5% and 2.2%, respectively.

The uncertainty in the line shape of the cross sections can introduce systematic uncertainties in both the ISR correction factor and the signal efficiency. To account for this, the measured cross sections are fitted with a cubic polynomial to obtain an updated line shape. This updated shape is then incorporated into the calculation of the ISR correction factors and efficiencies. The systematic uncertainty is assessed by comparing these results with those obtained using an alternative linear polynomial model, as shown in Fig. 5. The difference on the average cross section, 1.5% is taken as the systematic uncertainty.

The $D_s^\pm$ mass resolution discrepancy between data and MC simulation affects the efficiencies. The uncertainty due to the mass window for the $D_s^\pm \to K_S^0 K^\pm$ decay is assessed by varying the nominal mass window by ± 15 MeV$/c^2$. The relative difference between the observed cross sections and the nominal results, 2.2%, is taken as the systematic uncertainty. For the $D_s^\pm \to K^+ K^- \pi^\pm$ decay, the systematic uncertainty is taken to be 1% according to Ref. [49].

The systematic uncertainty associated with the signal yield encompasses uncertainties in the fitting range, the signal shape, and the background shape. The uncertainty related to the fitting range is evaluated using the Barlow test [50]. By varying the fit range, the changes in the final results consistently remain below 2σ, making this uncertainty negligible. To estimate the systematic uncertainty related to the $RM(\pi^+\pi^- D_s^\pm)$ signal shape, we account for the resolution difference between data and MC simulation. The nominal MC-derived shape is convolved with a Gaussian function [51]. The resulting difference in the signal yields, 6.4%, is taken as the systematic uncertainty. For the background shape, the uncertainty is estimated by replacing the first-order polynomial with a second-order polynomial, and the resulting difference in fitted signal yields is less than 0.1%, which is negligible.

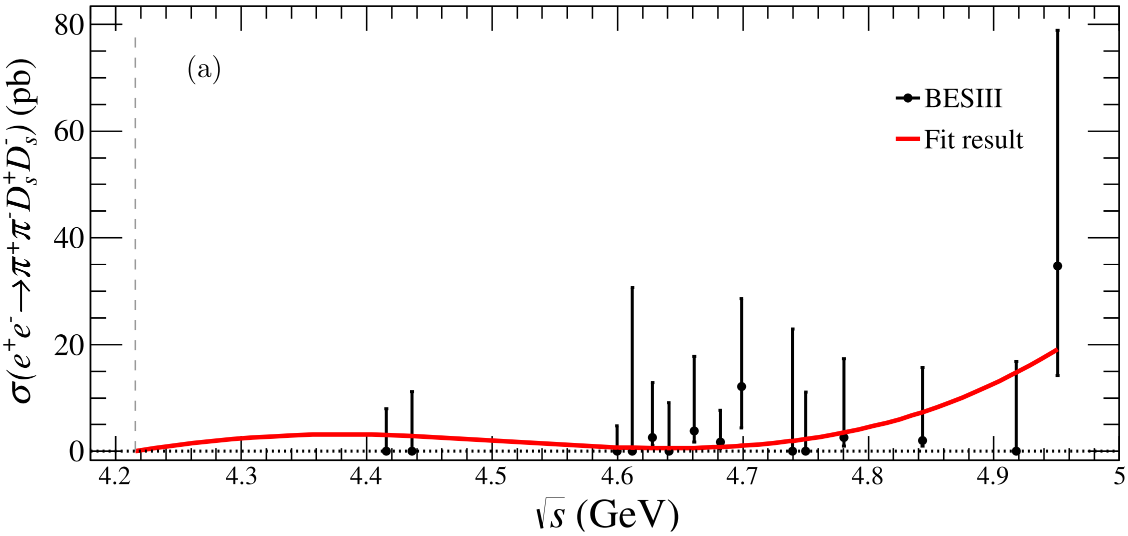

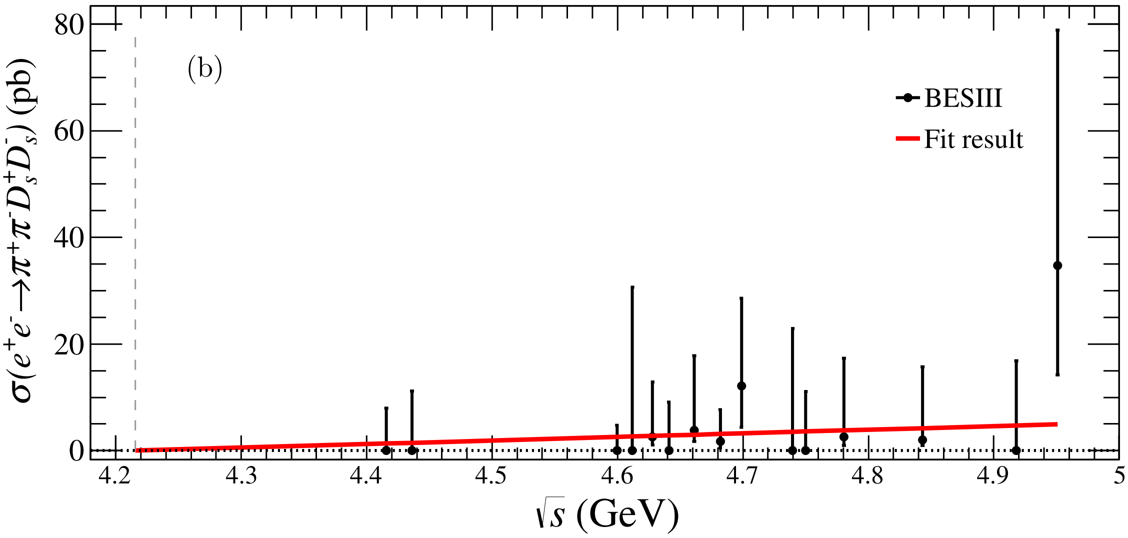

FIG 5. Born cross section line shapes for $e^+e^- \to \pi^+\pi^-D_s^+D_s^-$ fitted with (a) a cubic polynomial and (b) a linear polynomial.

8 Upper Limit With Systematic Uncertainty

Since the statistical significance is only 1.2σ, no significant $e^+e^- \to \pi^+\pi^-D_s^+D_s^-$ signals are observed, an upper limit at the 90% C.L. on the cross section is set using the Bayesian method. In this method, the probability distribution of the measured cross section σ, $P(\sigma)$, is determined using a maximum likelihood fit. The upper limit at the 90% confidence level (C.L.), denoted as L, is then calculated by solving the equation

$$0.1 = \int_L^\infty P(\sigma)d\sigma. \tag{8.1}$$

To include multiplicative systematic uncertainties from tracking, integrated luminosity, PID, branching fractions, and the ISR correction factor, $P(\sigma)$ is convolved with a probability distribution function of sensitivity, which refers to the denominator of Eq. (6.2) and

TABLE 1. Systematic uncertainties for the Born cross section (%).

Source	Uncertainty (%)
Integrated luminosity	1.0
Tracking	7.0
PID	7.0
K_S^0 reconstruction	0.4
$\mathcal{B}(D_s^+ \to K_S^0 K^+)$	0.6
$\mathcal{B}(D_s^+ \to K^+ K^- \pi^+)$	2.2
ISR correction factor	1.5
Mass window of $D_s^\pm \to K_S^0 K^\pm$	2.2
Mass window of $D_s^\pm \to K^+ K^- \pi^\pm$	1.0
Fit method	6.4
Total uncertainty	12.4

is assumed to be a Gaussian with the central value $\hat{S}$ and the standard deviation σ_s [52]. The convolution is performed as:

$$P'(\sigma) = \int_0^\infty P\left(\frac{S}{\hat{S}}\sigma\right) \exp\left[-\frac{(S-\hat{S})^2}{2\sigma_s^2}\right] dS, \tag{8.2}$$

where $P(\sigma)$ is the likelihood distribution obtained from fitting the likelihood of the number of signal events and parameterized as three Gaussians. The sensitivity is denoted by $\hat{S}$, and its multiplicative systematic uncertainty is σ_s. Finally, the upper limit at the 90% C.L. is obtained by integrating $P'(\sigma)$ rather than $P(\sigma)$ in Eq. (8.1). Figure 6 shows the likelihood distribution before and after convolution at the energy of 4.70 GeV.

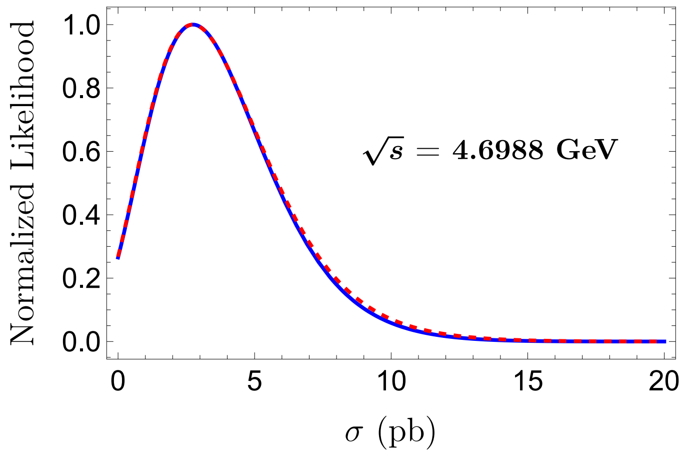

FIG 6. The likelihood distribution before (blue line) and after (red line) convolution.

9 Summary

In this work, we report the study of the process $e^+e^- \to \pi^+\pi^- D_s^+ D_s^-$ at c.m. energies from 4.42 to 4.95 GeV using BESIII data. No significant signals are observed in this region. The Born cross sections are measured at fifteen energy values, and the corresponding upper limits at the 90% C.L. are determined after considering the systematic uncertainties. These results are listed in TABLE 2. To further investigate the charm-strange quark dynamics and search for potential multi-quark structures, the $M(D_s^+ D_s^-)$ invariant mass spectrum was examined. No significant resonant structures are observed, with the present data set, underscoring the need for higher statistics in future investigations of this channel.

TABLE 2. The results of the Born cross sections for $e^+e^- \to \pi^+\pi^- D_s^+ D_s^-$. The table includes the integrated luminosity $\mathcal{L}$, the number of signal events $N^{\rm obs}$, the ISR correction factor $(1+\delta^r)$ and the VP correction factor $(1+\delta^v)$, the sum of the products of the branching fraction and efficiency $\sum_{i,j} \epsilon_{ij}\mathcal{B}_i\mathcal{B}_j$, and the Born cross section σ along with its upper limit at the 90% C.L. The first and second uncertainties are statistical and systematic.

$\sqrt{s}$ (GeV)	$\mathcal{L}$ (pb^{-1})	$N^{\rm sig}$	$\sum_{i,j} \epsilon_{ij}\mathcal{B}_i\mathcal{B}_j$ (10^{-4})	$(1+\delta^r)\times$ $(1+\delta^v)$	σ $(\sigma_{\rm UL})$ (pb)
4.4156	1043.9	$0.0^{+2.2}_{-0.0}$	2.871	0.863	$0.0^{+8.2}_{-0.0} \pm 0.0$ (<13.8)
4.4362	569.9	$0.0^{+1.8}_{-0.0}$	2.933	0.896	$0.0^{+11.5}_{-0.0} \pm 0.0$ (<21.1)
4.5995	586.9	$0.0^{+1.2}_{-0.0}$	3.296	0.975	$0.0^{+4.9}_{-0.0} \pm 0.0$ (<9.7)
4.6119	103.6	$0.0^{+1.2}_{-0.0}$	2.796	0.995	$0.0^{+31.5}_{-0.0} \pm 0.0$ (<62.5)
4.6280	521.5	$0.5^{+2.0}_{-0.3}$	2.738	1.001	$2.6^{+10.5}_{-1.6} \pm 0.3$ (<21.1)
4.6409	551.6	$0.0^{+1.9}_{-0.0}$	2.812	1.008	$0.0^{+9.4}_{-0.0} \pm 0.0$ (<16.9)
4.6612	529.4	$0.7^{+2.6}_{-0.4}$	2.795	1.014	$3.9^{+14.3}_{-2.2} \pm 0.5$ (<26.8)
4.6819	1667.4	$1.0^{+3.4}_{-0.7}$	3.052	1.018	$1.8^{+6.1}_{-1.2} \pm 0.2$ (<11.3)
4.6988	535.5	$2.2^{+3.0}_{-1.4}$	3.242	1.018	$12.4^{+17.0}_{-7.9} \pm 1.5$ (<39.6)
4.7397	163.9	$0.0^{+1.4}_{-0.0}$	4.043	1.006	$0.0^{+23.5}_{-0.0} \pm 0.0$ (<46.9)
4.7501	366.5	$0.0^{+1.5}_{-0.0}$	4.086	1.000	$0.0^{+11.4}_{-0.0} \pm 0.0$ (<22.7)
4.7805	511.5	$0.5^{+2.8}_{-0.3}$	4.253	0.979	$2.7^{+15.1}_{-1.6} \pm 0.3$ (<28.0)
4.8431	525.2	$0.4^{+2.8}_{-0.2}$	4.510	0.931	$2.0^{+14.1}_{-1.0} \pm 0.2$ (<25.1)
4.9180	207.8	$0.0^{+1.4}_{-0.0}$	4.609	0.891	$0.0^{+17.3}_{-0.0} \pm 0.0$ (<34.7)
4.9509	159.3	$2.2^{+2.8}_{-1.3}$	4.667	0.865	$35.7^{+45.4}_{-21.1} \pm 4.4$ (<108.9)

Acknowledgments

The BESIII Collaboration thanks the staff of BEPCII (https://cstr.cn/31109.02.BEPC) and the IHEP computing center for their strong support. This work is supported in part by National Key R&D Program of China under Contracts Nos. 2023YFA1606704, 2025YFA1613900, 2023YFA1606000; National Natural Science Foundation of China (NSFC) under Contracts Nos. 11635010, 11935015, 11935016, 11935018, 12025502, 12035009, 12035013, 12061131003, 12192260, 12192261, 12192262, 12192263, 12192264, 12192265, 12221005, 12225509, 12235017, 12342502, 12361141819, 12535005, 12575089; the Chinese Academy of Sciences (CAS) Large-Scale Scientific Facility Program; the Strategic Priority Research Program of Chinese Academy of Sciences under Contract No. XDA0480600; CAS under Contract No. YSBR-101; 100 Talents Program of CAS; The Institute of Nuclear and Particle Physics (INPAC) and Shanghai Key Laboratory for Particle Physics and Cosmology; ERC under Contract No. 758462; German Research Foundation DFG under Contract No. FOR5327; Istituto Nazionale di Fisica Nucleare, Italy; Knut and Alice Wallenberg Foundation under Contracts Nos. 2021.0174, 2021.0299, 2023.0315; Ministry of Development of Turkey under Contract No. DPT2006K-120470; National Research Foundation of Korea under Contract No. NRF-2022R1A2C1092335; National Science and Technology fund of Mongolia; Polish National Science Centre under Contract No. 2024/53/B/ST2/00975; STFC (United Kingdom); Swedish Research Council under Contract No. 2019.04595; U. S. Department of Energy under Contract No. DE-FG02-05ER41374.

References

[1] B. Aubert *et al.* (BABAR Collaboration), Phys. Rev. Lett. **95**, 142001 (2005).

[2] B. Aubert *et al.* (BABAR Collaboration), Phys. Rev. Lett. **98**, 212001 (2007).

[3] J. P. Lees *et al.* (BABAR Collaboration), Phys. Rev. D **86**, 051105(R) (2012).

[4] J. P. Lees *et al.* (BABAR Collaboration), Phys. Rev. D **89**, 111103(R) (2014).

[5] X. L. Wang *et al.* (Belle Collaboration), Phys. Rev. Lett. **99**, 142002 (2007).

[6] C. Z. Yuan *et al.* (Belle Collaboration), Phys. Rev. Lett. **99**, 182004 (2007).

[7] Z. Q. Liu *et al.* (Belle Collaboration), Phys. Rev. Lett. **110**, 252002 (2013).

[8] X. L. Wang *et al.* (Belle Collaboration), Phys. Rev. D **91**, 112007 (2015).

[9] T. Coan *et al.* (CLEO Collaboration), Phys. Rev. Lett. **96**, 162003 (2006).

[10] Q. He *et al.* (CLEO Collaboration), Phys. Rev. D **74**, 091104(R) (2006).

[11] C. Z. Yuan, Chin. Phys. C **38**, 043001 (2014).

[12] M. Ablikim *et al.* (BESIII Collaboration), Phys. Rev. Lett. **114**, 092003 (2015).

[13] M. Ablikim *et al.* (BESIII Collaboration), Phys. Rev. D **91**, 112005 (2015).

[14] S. L. Zhu, Phys. Lett. B **625**, 212 (2005); F. E. Close and P. R. Page, Phys. Lett. B **628**, 215 (2005); E. Kou and O. Pene, Phys. Lett. B **631**, 164 (2005).

[15] L. Maiani, V. Riquer, F. Piccinini, and A. D. Polosa, Phys. Rev. D **72**, 031502(R) (2005).

[16] X. Liu, X. Q. Zeng, and X. Q. Li, Phys. Rev. D **72**, 054023(R) (2005).

[17] X. Wang, X. Liu, and Y. Gao, Rev. Mod. Phys. **98** (2026) (in press), arXiv:2502.15117.

[18] M. Ablikim *et al.* (BESIII Collaboration), Phys. Rev. Lett. **122**, 102002 (2019).

[19] M. Ablikim *et al.* (BESIII Collaboration), Phys. Rev. Lett. **112**, 022001 (2014).

[20] M. Ablikim *et al.* (BESIII Collaboration), Phys. Rev. Lett. **126**, 102001 (2021).

[21] R. Aaij *et al.* (LHCb Collaboration), Phys. Rev. Lett. **131**, 071901 (2023).

[22] M. Ablikim *et al.*, Chin. Phys. C **46**, 113002 (2022).

[23] M. Ablikim *et al.*, Chin. Phys. C **46**, 113003 (2022).

[24] S. Prelovsek, S. Collins, D. Mohler, M. Padmananth and S. Piemonte, J. High Energy Phys. **06**, 035 (2021).

[25] X. Liu, H. Huang, J. Ping, D. Chen and X. Zhu, Eur. Phys. J. C **81**, 950 (2021).

[26] M. Ablikim *et al.* (BESIII Collaboration), Nucl. Instrum. Methods Phys. Res., Sect. A **614**, 345 (2010).

[27] C. H. Yu *et al.*, Proceedings of IPAC 2016, Busan, Korea (2016).

[28] M. Ablikim *et al.* (BESIII Collaboration), Chin. Phys. C **44**, 040001 (2020).

[29] J. Lu, Y. Xiao, and X. Ji, Radiat. Detect. Technol. Methods **4**, 337 (2020).

[30] J. W. Zhang, L. H. Wu, S. S. Sun *et al.*, Radiat. Detect. Technol. Methods **6**, 289 (2022).

[31] X. Li *et al.*, Radiat. Detect. Technol. Methods **1**, 13 (2017).

[32] Y. X. Guo *et al.*, Radiat. Detect. Technol. Methods **1**, 15 (2017).

[33] P. Cao *et al.*, Nucl. Instrum. Methods Phys. Res., Sect. A **953**, 163053 (2020).

[34] W. D. Li, H. M. Liu *et al.*, Proceedings of CHEP06, Mumbai, India (2006).

[35] S. Agostinelli *et al.* (GEANT4 Collaboration), Nucl. Instrum. Methods Phys. Res., Sect. A **506**, 250 (2003).

[36] S. Jadach, B. F. L. Ward, and Z. Was, Phys. Rev. D **63**, 113009 (2001); Comput. Phys. Commun. **130**, 260 (2000).

[37] D. J. Lange, Nucl. Instrum. Methods Phys. Res., Sect. A **462**, 152 (2001).

[38] R. G. Ping, Chin. Phys. C **32**, 599 (2008).

[39] S. Navas *et al.* (Particle Data Group), Phys. Rev. D **110**, 030001 (2024).

[40] J. C. Chen, G. S. Huang, X. R. Qi, D. H. Zhang, and Y. S. Zhu, Phys. Rev. D **62**, 034003 (2000).

[41] D. J. Lange, Nucl. Instrum. Methods Phys. Res., Sect. A **462**, 152 (2001).

[42] E. A. Kuraev and V. S. Fadin, Sov. J. Nucl. Phys. **41**, 466 (1985) [Yad. Fiz. **41**, 733 (1985)].

[43] S. Actis *et al.*, Eur. Phys. J. C **66**, 585 (2010).

[44] M. Ablikim *et al.* (BESIII Collaboration), Chin. Phys. C **39**, 093001 (2015).

[45] W. L. Yuan, X. C. Ai, X. B. Ji, S. J. Chen, Y. Zhang, L. H. Wu, L. L. Wang, and Y. Yuan, Chin. Phys. C **40**, 026201 (2016).

[46] M. Ablikim *et al.* (BESIII Collaboration), Phys. Rev. D **86**, 092009 (2012).

[47] M. Ablikim *et al.* (BESIII Collaboration), Phys. Rev. D **83**, 112005 (2011).

[48] M. Ablikim *et al.* (BESIII Collaboration), Phys. Rev. D **110**, 032017 (2024).

[49] M. Ablikim *et al.* (BESIII Collaboration), Phys. Rev. Lett. **131**, 151903 (2023).

[50] O. Behnke, K. Kroninger, G. Schott, and T. H. Schorner-Sadenius, Wiley-VCH, Berlin, Germany, 2013.

[51] M. Ablikim *et al.* (BESIII Collaboration), Phys. Rev. Lett. **135**, 071901 (2025).

[52] K. Stenson, arXiv:physics/0605236.